Cell, Vol. 99, 247–257, October 29, 1999, Copyright ©1999 by Cell Press

DNA Methyltransferases Dnmt3a and Dnmt3b Are Essential for De Novo Methylation and Mammalian Development

Masaki Okano,* Daphne W. Bell,† Daniel A. Haber,† and En Li*‡

*Cardiovascular Research Center
†Cancer Center
Massachusetts General Hospital
Department of Medicine
Harvard Medical School
Charlestown, Massachusetts 02129

Summary

The establishment of DNA methylation patterns requires de novo methylation that occurs predominantly during early development and gametogenesis in mice. Here we demonstrate that two recently identified DNA methyltransferases, Dnmt3a and Dnmt3b, are essential for de novo methylation and for mouse development. Inactivation of both genes by gene targeting blocks de novo methylation in ES cells and early embryos, but it has no effect on maintenance of imprinted methylation patterns. Dnmt3a and Dnmt3b also exhibit nonoverlapping functions in development, with Dnmt3b specifically required for methylation of centromeric minor satellite repeats. Mutations of human *DNMT3B* are found in ICF syndrome, a developmental defect characterized by hypomethylation of pericentromeric repeats. Our results indicate that both Dnmt3a and Dnmt3b function as de novo methyltransferases that play important roles in normal development and disease.

Introduction

Covalent modification of DNA by methylation of cytosine residues is a heritable and reversible epigenetic process, which is involved in regulation of a diverse range of biological processes in vertebrate animals, plants, and fungi (reviewed by Colot and Rossignol, 1999). In mammals, DNA methylation is essential for normal embryonic development (reviewed by Li, 1997), and it plays important roles in the regulation of gene expression, X chromosome inactivation, genomic imprinting, chromatin modification, and silencing of endogenous retroviruses (for reviews, see Jähner and Jaenisch, 1984; Brockdorff, 1997; Surani, 1998; Ng and Bird, 1999). Altered DNA methylation patterns have been implicated in tumorigenesis (reviewed by Ehrlich, 1999; Jones and Laird, 1999).

DNA methylation changes in a highly orchestrated way during mouse development, involving genome-wide as well as gene-specific demethylation and de novo methylation (reviewed by Razin and Cedar, 1993). The fertilized egg first undergoes a wave of demethylation during preimplantation development, which erases part of the inherited parental methylation pattern. The DNA of blastocysts is thus relatively undermethylated. After implantation, the embryo undergoes a wave of de novo methylation that establishes a new embryonic methylation pattern (Monk et al., 1987; Sanford et al., 1987; Howlett and Reik, 1991; Kafri et al., 1992). The biological function of this dynamic reprogramming of DNA methylation in early development is unknown. Demethylation and de novo methylation also occur during gametogenesis and have been shown to play a critical role in the establishment of parental-specific methylation marks in imprinted genes (Chaillet et al., 1991; Stöger et al., 1993; Tremblay et al., 1995).

Riggs (1975) and Holliday and Pugh (1975) first proposed that heritable DNA methylation provides a mechanism for the developmental regulation of gene expression. They predicted the existence of a maintenance methyltransferase that methylates unmethylated sites with great difficulty but easily methylates hemi-methylated sites. The existence of such maintenance methyltransferase activity was subsequently demonstrated by experiments showing the clonal inheritance of methylation patterns in mammalian cells (Wigler et al., 1981; Stein et al., 1982) and by the cloning of the first mammalian DNA methyltransferase, now known as *Dnmt1* (Bestor et al., 1988). Purified Dnmt1 protein methylates DNA containing hemimethylated CpG dinucleotides more efficiently than unmethylated DNA in vitro (Bestor, 1992). The Dnmt1 protein has been localized to DNA replication foci, suggesting that maintenance methylation might be coupled to DNA replication (Leonhardt et al., 1992). Further, inactivation of the mouse *Dnmt1* gene by gene targeting results in extensive demethylation of all sequences examined (Li et al., 1992; Lei et al., 1996). Together, these findings strongly suggest that Dnmt1 functions as a major maintenance methyltransferase in vivo, ensuring "replication" of DNA methylation patterns after each round of cell division.

De novo methylation activity is detected predominantly in early embryos and embryonic carcinoma (EC) cells (Jähner et al., 1982; Palmiter et al., 1982; Stewart et al., 1982). Although Dnmt1 can methylate unmethylated DNA in vitro, evidence for its involvement in de novo methylation during development remains sketchy. In contrast, genetic studies suggest that enzymes other than Dnmt1 might be responsible for de novo methylation in vivo, since ES cells completely lacking Dnmt1 are still capable of methylating retroviral DNA de novo (Lei et al., 1996). The search for the mammalian de novo methyltransferase has yielded several new methyltransferases, including members of the Dnmt2 and the Dnmt3 families. Although the Dnmt2 protein contains all the conserved motifs shared by known prokaryotic and eukaryotic DNA cytosine methyltransferases, inactivation of *Dnmt2* in mouse ES cells by gene targeting perturbs neither de novo methylation nor maintenance methylation of proviral DNA, making it unlikely that Dnmt2 is the enzyme responsible for global de novo methylation (Okano et al., 1998a).

‡To whom correspondence should be addressed (e-mail: en@cvrc.mgh.harvard.edu).

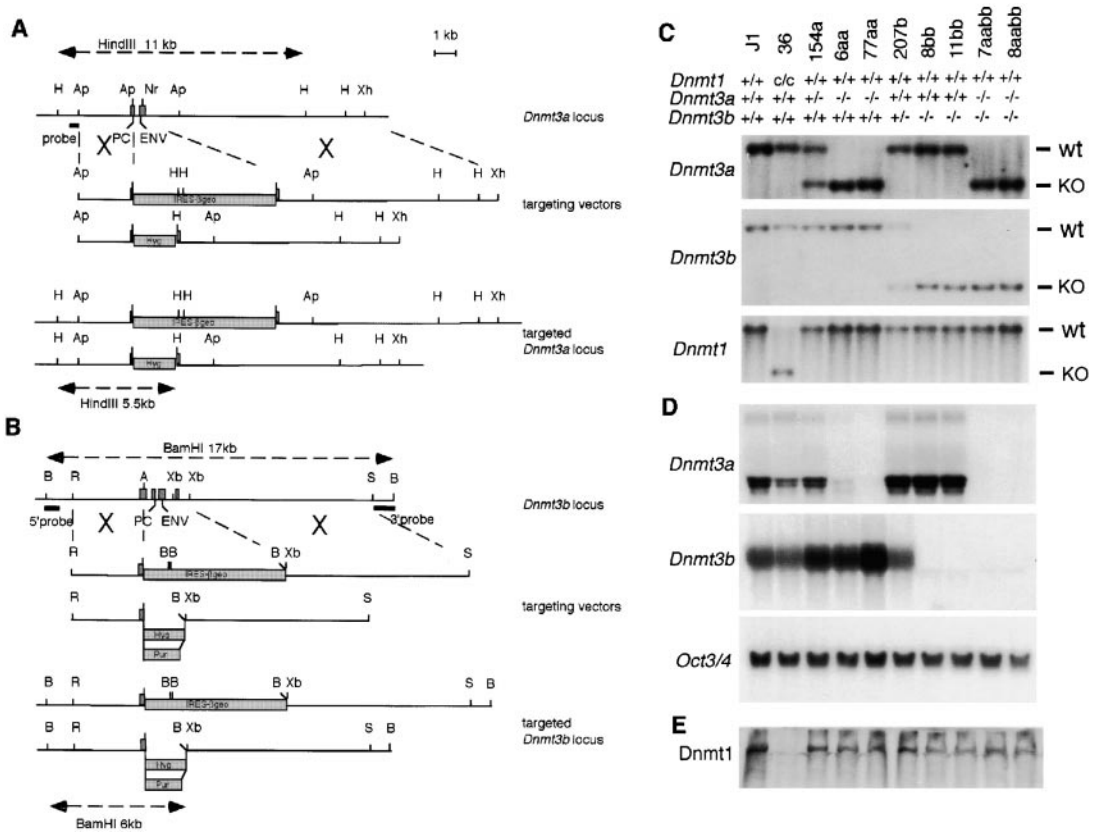

Figure 1. Targeted Disruption of *Dnmt3a* and *Dnmt3b*

(A and B) Gene targeting at the *Dnmt3a* locus (A) and *Dnmt3b* locus (B). The top lines represent the wild-type genomic DNA structures, which contain exons (shaded boxes) encoding the highly conserved motifs IV (PC) and VI (ENV). The middle lines represent various targeting vectors in which motifs IV and VI are deleted to create null mutations. The bottom lines represent the mutant loci resulting from homologous recombination between targeting vectors and wild-type loci. H, HindIII; Ap, ApaI; Nr, NruI; Xh, XhoI; B, BamHI; R, EcoRV; A, AatII; Xb, XbaI; S, ScaI; Hyg, PGK-hygromycin cassette; Pur, PGK-puromycin cassette.

(C–E) Establishment of the mutant ES cell lines. J1, a wild-type line; 36, a *Dnmt1* null mutant line (Lei et al., 1996); 154a, a *Dnmt3a* heterozygous line; 6aa, a *Dnmt3a* homozygous mutant line (βgeo/hyg); 77aa, a *Dnmt3a* homozygous mutant line (βgeo/βgeo); 207b, a *Dnmt3b* heterozygous line; 8bb and 11bb, independent *Dnmt3b* homozygous lines (βgeo/hyg); 7aabb and 8aabb, independent lines homozygous for both *Dnmt3a* (βgeo/βgeo) and *Dnmt3b* (hyg/puro) mutations (derived from 77aa). (C) Southern analysis of the genotype of mutant lines. Genomic DNA was digested with HindIII (*Dnmt3a*), BamHI (*Dnmt3b*), or EcoRV (*Dnmt1*). wt, wild-type alleles; KO, mutant alleles. (D) Northern analysis of total RNA (20 μg per lane) from wild-type and mutant ES cells. The same blot was hybridized repeatedly with cDNA probes for *Dnmt3a*, *Dnmt3b*, or *Oct3/4*. It should be noted that smaller and faint transcripts derived from the PGK-hygromycin targeted allele of *Dnmt3a* were detected from line 6aa, which was not used for generation of the double mutant ES cells and mice. (E) Immunoblot analysis with anti-Dnmt1 antibodies. All cell lines except *Dnmt1* null ES cells (c/c) expressed Dnmt1 protein.

The murine *Dnmt3* family consists of two genes, *Dnmt3a* and *Dnmt3b*, which are highly expressed in undifferentiated ES cells but downregulated after differentiation and expressed at low levels in adult somatic tissues (Okano et al., 1998b). We have previously shown that recombinant Dnmt3a and Dnmt3b proteins methylate CpG dinucleotides in various native and synthetic DNA substrates and show no preference for hemimethylated DNA (Okano et al., 1998b). These results raised the possibility that *Dnmt3a* and *Dnmt3b* encode the long-sought de novo methyltransferases, known to be highly active in ES cells and early embryos. To test this hypothesis, we inactivated both genes by gene targeting in ES cells and mice. We show here that both Dnmt3a and Dnmt3b are required for genome-wide de novo methylation and are essential for mammalian development.

Results

Inactivation of Both *Dnmt3a* and *Dnmt3b* Disrupts De Novo Methylation in ES Cells

Since both *Dnmt3a* and *Dnmt3b* encode functional DNA methyltransferases with similar biochemical properties and both genes are expressed at high levels in ES cells (Okano et al., 1998b), we speculated that Dnmt3a and Dnmt3b might have overlapping functions. To test this hypothesis, we inactivated *Dnmt3a*, *Dnmt3b*, or both genes (four alleles) in ES cells by gene targeting. Several gene targeting vectors were constructed by deletion of part of the catalytic domain containing the highly conserved PC and ENV motifs (motifs IV and VI) (reviewed by Kumar et al., 1994) and by insertion of different selection markers, including the IRES-βgeo, PGK-hygromycin, and PGK-puromycin cassettes (Figures 1A

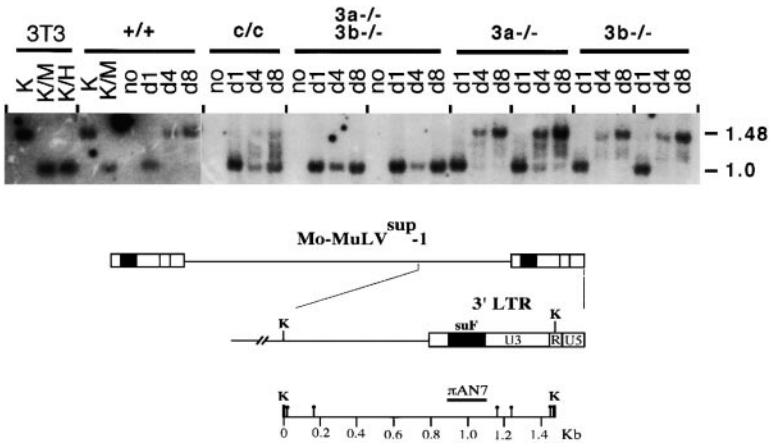

Figure 2. Disruption of De Novo Methylation of Proviral DNA in ES Cells Homozygous for Both *Dnmt3a* and *Dnmt3b* Mutations

Genomic DNA was isolated from ES cells 1, 4, or 8 days after infection with MoMuLV^{sup}-1 retrovirus (d1, d4, and d8), or before infection (no), and digested with KpnI and HpaII. The methylation status of newly integrated MoMuLV^{sup}-1 proviral DNA was analyzed by Southern hybridization using the *supF* probe, πAN7. The 1.48 kb Kpn I (K) fragment in the 3′ LTR region contains five HpaII/MspI sites (lollipops) as shown in the lower panel. KpnI (K) digestion yields a 1.48 kb band, which represents complete methylation, while double digestion with KpnI and MspI (K/M) yields a 1.0 kb band, which represents unmethylated status. Cell lines: *3T3*, NIH3T3; +/+, wild type ES cells; c/c, *Dnmt1* null mutant ES cells; 3a$^{-/-}$ 3b$^{-/-}$, *Dnmt3a* and *Dnmt3b* double homozygous lines, 7aabb and 8aabb; 3a$^{-/-}$, *Dnmt3a* homozygous lines, 6aa and 77aa; and 3b$^{-/-}$, *Dnmt3b* homozygous lines, 8bb and 11bb. Note that de novo methylation of proviral DNA was completely blocked in cells lacking both Dnmt3a and Dnmt3b.

and 1B; and see Experimental Procedures). Since missense mutations of the PC motifs result in complete inactivation of DNA methyltransferase activities (Kumar et al., 1994), we predicted that our deletion mutations would be functionally null.

ES cell lines homozygous for single gene disruption (*Dnmt3a*$^{-/-}$ or *Dnmt3b*$^{-/-}$) or for mutations of both genes ([*Dnmt3a*$^{-/-}$, *Dnmt3b*$^{-/-}$]) were successfully isolated (Figure 1C, see Experimental Procedures). Northern analysis using cDNA probes corresponding to the catalytic domain did not detect any stable transcripts from *Dnmt3a* and *Dnmt3b* targeted loci, indicating that the catalytic domain was not expressed from the mutant genes (Figure 1D). All homozygous ES cell lines retained undifferentiated morphology and expressed *Oct3/4*, an undifferentiated ES cell marker (Figure 1D). We also showed that Dnmt1 protein was expressed at approximately the same levels in all *Dnmt3* mutant cell lines as in wild-type cells (Figure 1E).

Proviral DNA derived from new retroviral infection is actively methylated de novo in EC and ES cells (Stewart et al., 1982; Lei et al., 1996). To examine whether ES cells lacking Dnmt3a, Dnmt3b, or both enzymes have de novo methylation activity, we infected these ES cell lines with a recombinant retrovirus, MoMuLV^{sup}-1 (Figure 2, lower panel), and analyzed the methylation status of proviral DNA using the CpG methylation-sensitive enzyme HpaII. We showed that the unmethylated 1.0 kb band was shifted to the fully methylated 1.48 kb band in wild-type ES cells over a period of 8 days, indicative of active de novo methylation, but remained unmethylated in NIH3T3 cells, known to have low de novo methyltransferase activity (Figure 2). As shown previously, the proviral DNA was partially methylated in *Dnmt1* null mutant ES cells (c/c), demonstrated by the presence of multiple bands ranging from 1.0 kb to 1.48 kb (Figure 2) (Lei et al., 1996). Although *Dnmt3a*$^{-/-}$ or *Dnmt3b*$^{-/-}$ single mutant ES cell lines methylate proviral DNA normally, the [*Dnmt3a*$^{-/-}$, *Dnmt3b*$^{-/-}$] double mutant ES cells completely lacked de novo methylation activity (Figure 2). These results demonstrate that Dnmt3a and Dnmt3b are essential for de novo methylation in ES cells, and that these two gene products are redundant in this function.

Dnmt3a and Dnmt3b Are Essential for Embryonic Development

To determine whether Dnmt3a and Dnmt3b are also required for de novo methylation during embryonic development, we generated Dnmt3-deficient mice from multiple ES cell lines heterozygous for either *Dnmt3a* or *Dnmt3b* mutations. We first determined the expression patterns of *Dnmt3a* and *Dnmt3b* during early development, taking advantage of the fact that both *Dnmt3a* and *Dnmt3b* mutant genes were tagged by insertion of the IRES-βgeo cassette (Figures 1A and 1B). The expression pattern of *Dnmt3* genes could thus be determined by analyzing the *lacZ* expression pattern from the *Dnmt3*-IRES-βgeo fusion gene (Mountford et al., 1994). We showed by X-gal staining of heterozygous embryos that *Dnmt3a* was moderately expressed in embryonic ectoderm and weakly in mesodermal cells of E7.5 embryos (Figures 3A and 3B). At E8.5 and E9.5, *Dnmt3a* expression became ubiquitous with increased expression in the somites and the ventral part of the embryo (Figures 3C and 3D). *Dnmt3b*, on the other hand, was highly expressed in the embryonic ectoderm, neural ectoderm, and chorionic ectoderm at E7.5, although weak expression was also detected in mesodermal and endodermal cells (Figures 3E and 3F). At later stages, *Dnmt3b* expression was detected predominantly in the forebrain and eyes but weakly throughout the embryo (Figures 3G and 3H). It is noteworthy that in early embryos *Dnmt3a* and *Dnmt3b* show overlapping expression in the embryonic ectoderm, with *Dnmt3b* expressed at higher levels than *Dnmt3a*, suggestive of possible overlapping functions.

Both *Dnmt3a*$^{+/-}$ and *Dnmt3b*$^{+/-}$ heterozygous mice were grossly normal and fertile. *Dnmt3a*$^{-/-}$ and *Dnmt3b*$^{-/-}$ mice were then derived by intercrosses of heterozygous mice. *Dnmt3a*$^{-/-}$ mice developed to term and appeared to be normal at birth. However, most homozygous mutant mice became runted and died at about 4 weeks of age (Figure 4A). In contrast, no viable

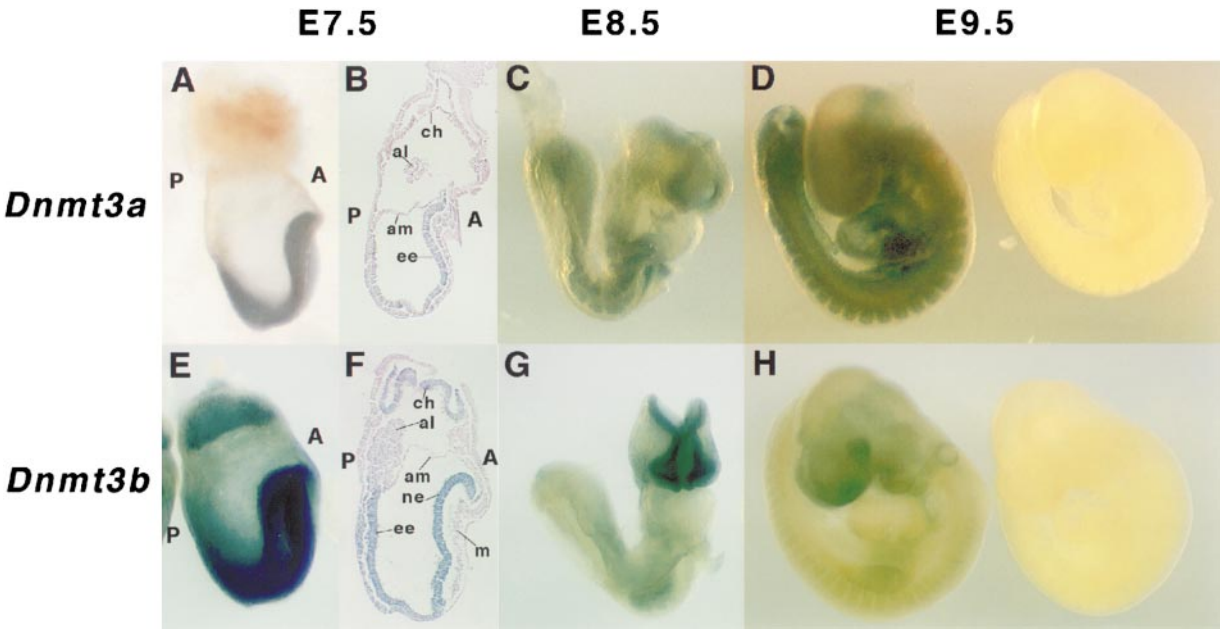

Figure 3. The Expression Patterns of *Dnmt3a* and *Dnmt3b* during Early Embryonic Development

Whole-mount X-gal staining of *Dnmt3a*$^{+/-}$ embryos (A–D) or *Dnmt3b*$^{+/-}$ embryos (E–H), which carry the IRES-βgeo marker driven by the endogenous *Dnmt3a* or *Dnmt3b* promoter, respectively. Embryos were dissected out at E7.5 (A, B, E, and F), E8.5 (C and G), and E9.5 (D and H). Sagittal sections of E7.5 embryos after X-gal staining (B and F) reveal overlapping expression of *Dnmt3a* and *Dnmt3b* in the embryonic ectoderm and distinct expression of *Dnmt3b* in the chorion. The expression of *Dnmt3a* appears to be ubiquitous at E8.5 and E9.5, whereas *Dnmt3b* is expressed at high levels in the anterior head region and eyes. The unstained embryos on the right in (D) and (H) are wild-type littermates. A, anterior; P, posterior; al, allantois; am, amnion; ch, chorion; ee, embryonic ectoderm; m, mesoderm; and ne, neuroectoderm.

Dnmt3b$^{-/-}$ mice were recovered at birth. Dissection of embryos at different stages of development revealed that *Dnmt3b*$^{-/-}$ embryos had multiple developmental defects including growth impairment and rostral neural tube defects with variable severity at later stages of development (Figures 4B and 4C), though most of them appeared to develop normally before E9.5. The detailed tissue and cellular defects in *Dnmt3a*$^{-/-}$ and *Dnmt3b*$^{-/-}$ mice are under investigation.

To test whether *Dnmt3a* and *Dnmt3b* might have overlapping function during early embryonic development, we analyzed the phenotypes of offspring derived from intercrosses of [*Dnmt3a*$^{+/-}$, *Dnmt3b*$^{+/-}$] compound heterozygous mice. After dissection and genotype analysis of 198 embryos, we found that all [*Dnmt3a*$^{-/-}$, *Dnmt3b*$^{-/-}$] double homozygous embryos (n = 5, expecting 1/16 of total offspring) showed smaller size and abnormal morphology at E8.5 and E9.5 and died before E11.5 (Figures 4E and 4H). The [*Dnmt3a*$^{-/-}$, *Dnmt3b*$^{-/-}$] embryos lacked somites and did not undergo embryonic turning, indicating that their growth and morphogenesis were arrested shortly after gastrulation (Figure 4E). These embryonic defects are very similar to those of *Dnmt1* null mutant embryos (Figure 4F) (Lei et al, 1996) but evidently more severe than those of *Dnmt3a*$^{-/-}$ or *Dnmt3b*$^{-/-}$ single mutant mice. Our results thus demonstrate that Dnmt3a and Dnmt3b have overlapping functions during early embryogenesis.

De Novo Methylation Is Impaired in [*Dnmt3a*$^{-/-}$, *Dnmt3b*$^{-/-}$] Embryos

To investigate whether the *Dnmt3* mutant embryos are defective in de novo methylation, we examined global genomic methylation patterns in E9.5 *Dnmt3a*$^{-/-}$, *Dnmt3b*$^{-/-}$, and [*Dnmt3a*$^{-/-}$, *Dnmt3b*$^{-/-}$] mutant embryos. The endogenous C-type retroviruses and intracisternal A particle (IAP) repeats at copy numbers of about 100 and 1000 per haploid genome, respecitvely, are known to be interspersed in the mouse genome and methylated at high levels in embryos and adult tissues (Sanford et al., 1987; Howlett and Reik, 1991; Li et al., 1992). We found that the endogenous C-type retroviral DNA was methylated at normal levels in *Dnmt3a*$^{-/-}$ embryos, but slightly undermethylated in *Dnmt3b*$^{-/-}$ embryos, and highly undermethylated in [*Dnmt3a*$^{-/-}$, *Dnmt3b*$^{-/-}$] embryos (Figure 5A). Nevertheless, a significant amount of methylation was retained in [*Dnmt3a*$^{-/-}$, *Dnmt3b*$^{-/-}$] embryos when compared to *Dnmt1* null mutant embryos, which lose almost all methylation (Lei et al., 1996) (Figure 5A). Similar results were obtained when the methylation status of the IAP repeats was examined (Figure 5B). In contrast to hypomethylation of these repetitive sequences, methylation of the 5′ upstream region of the imprinted gene *H19* was unaffected in [*Dnmt3a*$^{-/-}$, *Dnmt3b*$^{-/-}$] embryos (Figure 5C). This result is consistent with the observation that this region of *H19* is subject to neither demethylation nor de novo methylation during early embryogenesis (Tremblay et al., 1995).

To further determine whether the loss of methylation in repetitive sequences in [*Dnmt3a*$^{-/-}$, *Dnmt3b*$^{-/-}$] embryos was caused by impaired de novo methylation, we compared methylation levels between [*Dnmt3a*$^{-/-}$, *Dnmt3b*$^{-/-}$] embryos and blastocysts. We found that methylation levels of C-type retroviral DNA and the IAP

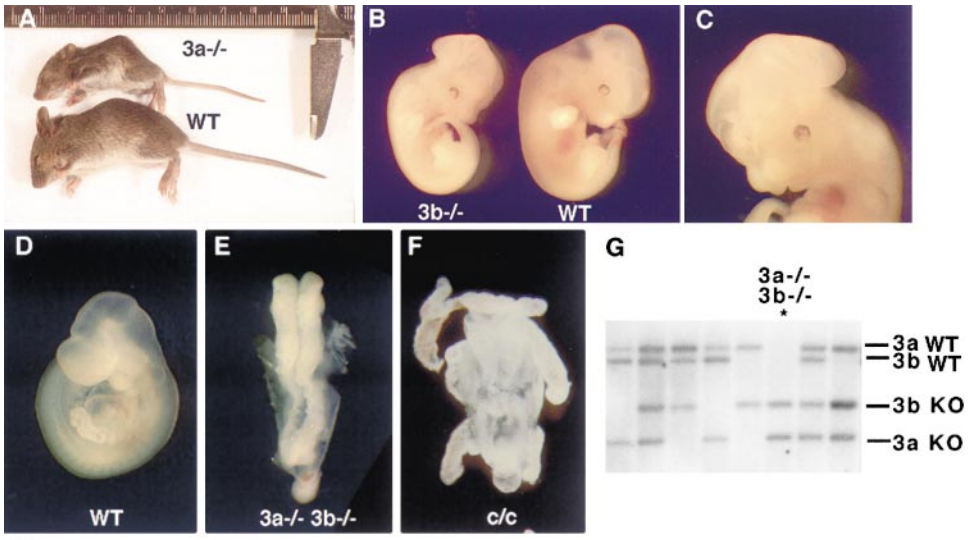

H

	Total	**3a-/- 3b-/-**	3a+/- 3b-/-	3a+/+ 3b-/-	3a-/- 3b+/-	3a+/- 3b+/-	3a+/+ 3b+/-	3a-/- 3b+/+	3a+/- 3b+/+	3a+/+ 3b+/+	Res
exp.ratio		**1**	2	1	2	4	2	1	2	1	
E8.5-9.5	119	**5(5)**	17(5)	6	13(1)	24(3)	14	8	11	5	16*
E11.5-15.5	79	**0**	3(3)	5(2)	8(2)	16(1)	10	1	16	5	15

Figure 4. Developmental Defects of *Dnmt3a* and *Dnmt3b* Single and Double Mutant Mice

(A) A *Dnmt3a*$^{-/-}$ mutant mouse and a wild-type littermate at 18 days after birth. (B) An E11.5 *Dnmt3b*$^{-/-}$ mutant embryo and its normal littermate. The enlarged head region of the mutant embryo shows rostral neural defects (C). (D) Side view of an E9.5 wild-type embryo. (E) Dorsal view of an E9.5 [*Dnmt3a*$^{-/-}$, *Dnmt3b*$^{-/-}$] embryo at the same magnification as (D). The [*Dnmt3a*$^{-/-}$, *Dnmt3b*$^{-/-}$] embryo was growth retarded and failed to turn and form somites and was morphologically indistinguishable from the *Dnmt1* null embryos (c/c) as shown in (F) (Lei et al. 1996). (G) Genotyping of one litter of E9.5 embryos by Southern hybridization. Genomic DNA was digested with BamHI and hybridized to the *Dnmt3a* probe and the *Dnmt3b* 3′ probe (Figures 1A and 1B) simultaneously. (H) Analysis of embryos derived from intercrosses of [*Dnmt3a*$^{+/-}$, *Dnmt3b*$^{+/-}$] compound heterozygous mice. Fourteen litters for E8.5–9.5 and eight litters for E11.5–15.5 were examined. Numbers in parenthesis represent the number of abnormal embryos. The mutant phenotypes include growth defects, neural defects, and others with variable penetrance. Res, resorbtion. (*) Of 16 resorbed embryos, 11 were collected from three litters, suggesting natural resorption due to abnormal pregnancy of the mother. All five double homozygous mutant embryos were growth arrested at the late gastrulation stage as shown in (E).

repeats in [*Dnmt3a*$^{-/-}$, *Dnmt3b*$^{-/-}$] embryos were essentially identical to those in blastocysts (Figures 5D and 5E). This result suggests that global methylation levels did not increase, and that de novo methylation did not occur in [*Dnmt3a*$^{-/-}$, *Dnmt3b*$^{-/-}$] embryos after implantation. In contrast, the methylation in C-type retroviral DNA and IAP repeats in E9.5 *Dnmt1* null mutant embryos was significantly lower than that in blastocysts (Figures 5D and 5E), indicating that inactivation of Dnmt1 resulted in demethylation of sequences which were methylated at the time of implantation. As summarized in Figure 5F, our results indicate that inactivation of both Dnmt3a and Dnmt3b blocks de novo methylation in early embryos but does not affect maintenance methylation of bulk genomic DNA. On the other hand, inactivation of Dnmt1 results in global demethylation, consistent with the fact that Dnmt1 is required for maintenance methylation.

Methylation of Repetitive Sequences and Imprinted Genes in *Dnmt3*-Deficient ES Cells

To determine whether inactivation of Dnm3a and Dnmt3b had any effect on global methylation of genomic DNA in ES cells, we examined the methylation status of a number of repetitive sequences and unique genes. We found that the dispersed C-type retroviruses and IAP repeats were slightly demethylated in [*Dnmt3a*$^{-/-}$, *Dnmt3b*$^{-/-}$] double homozygous lines, but in neither *Dnmt3a*$^{-/-}$ or *Dnmt3b*$^{-/-}$ single mutant lines nor two independent [*Dnmt3a*$^{-/-}$, *Dnmt3b*$^{+/-}$] lines isolated from the same experiment as the [*Dnmt3a*$^{-/-}$, *Dnmt3b*$^{-/-}$] mutant lines (Figures 6A and 6B). The major satellite DNA is composed of tandem repeats at copy numbers of 700,000 that are located in the centromeric region (Hastie, 1989). We showed that the major satellite DNA was also slightly demethylated in [*Dnmt3a*$^{-/-}$, *Dnmt3b*$^{-/-}$] mutant cells, but not in other *Dnmt3* mutant lines (Figure 6C). It should be noted that the repetitive elements in [*Dnmt3a*$^{-/-}$, *Dnmt3b*$^{-/-}$] cells were not demethylated as extensively as in cells homozygous for the *Dnmt1* mutations (Figures 6A–6C), indicating that Dnmt3a and Dnmt3b are involved, but do not play a major role, in keeping normal levels of methylation of repetitive sequences in ES cells.

We also examined the DNA methylation status of several imprinted genes and *Xist*, which had been

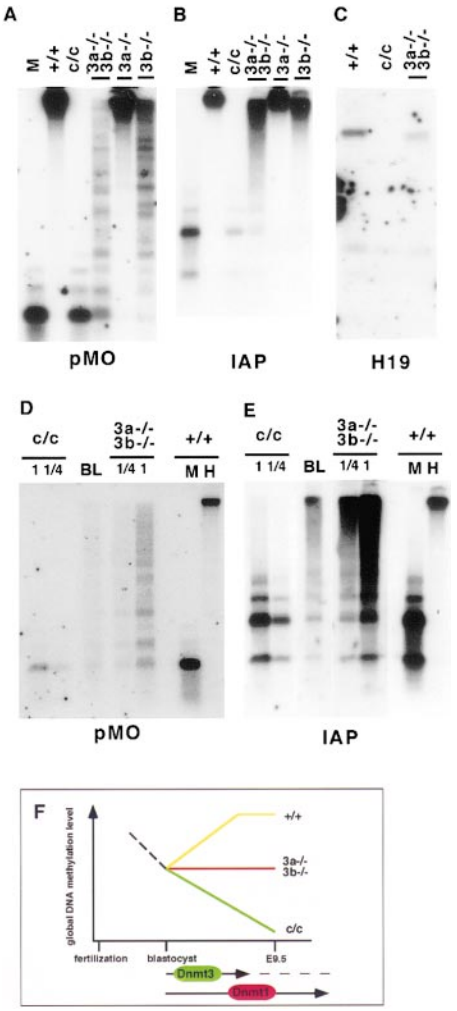

Figure 5. Disruption of De Novo Methylation but Not Maintenance Methylation in [*Dnmt3a*$^{-/-}$, *Dnmt3b*$^{-/-}$] Double Mutant Embryos

(A) Methylation of C-type retroviral DNA in E9.5 embryos. DNA was digested with HpaII or MspI (M) and probed with pMO. The genotype of embryos is indicated at the top as described in Figure 2.

(B) Methylation of IAP repeats in E9.5 embryos. DNA was digested with HpaII or MspI (M) and probed with the IAP probe.

(C) Methylation of the upstream region of *H19*. DNA was digested with SacI and HhaI and hybridized to the 5′ upstream probe.

(D and E) Comparison of methylation levels of C-type retrovirus (D) or IAP (E) in E9.5 [*Dnmt3a*$^{-/-}$, *Dnmt3b*$^{-/-}$] embryos, E9.5 *Dnmt1* null embryos (c/c), and blastocysts. DNA from E9.5 embryos was loaded at different quantities (1 or 1/4) for better comparison. DNA was digested with HpaII or MspI (M) and probed with pMO (D) or IAP (E). The methylation level in [*Dnmt3a*$^{-/-}$, *Dnmt3b*$^{-/-}$] embryos is comparable to that in blastocysts. In contrast, methylation levels in c/c embryos were lower than those in blastocysts. BL, blastocysts.

(F) Schematic diagram of methylation changes in wild-type (+/+), [*Dnmt3a*$^{-/-}$, *Dnmt3b*$^{-/-}$] double mutant (3a$^{-/-}$,3b$^{-/-}$), and *Dnmt1* null mutant embryos (c/c) during early development. During preimplantation development, the bulk DNA undergoes demethylation (dashed line), resulting in hypomethylation of genomic DNA at the blastocyst stage. After implantation of blastocysts, de novo methylation takes place, resulting in a rapid increase in methylation (yellow line). In [*Dnmt3a*$^{-/-}$, *Dnmt3b*$^{-/-}$] embryos, de novo methylation is impaired, but preexisting methylation patterns remain unaffected (red line), whereas in *Dnmt1* null mutants embryos, maintenance methylation is disrupted, resulting in rapid loss of methylation in all sequences (green line). This suggests that *Dnmt3a* and *Dnmt3b* encode de novo methyltransferases (green), while *Dnmt1* encodes a maintenance methyltransferase (red).

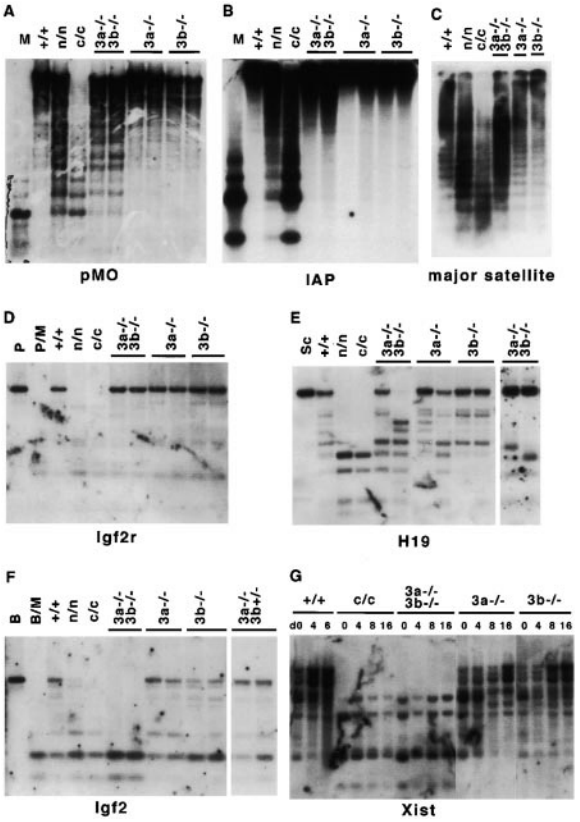

Figure 6. DNA Methylation in *Dnmt3a* and *Dnmt3b* Mutant ES Cells

(A–C) Genomic DNA from various ES cell lines as described in Figure 2 was digested with HpaII (A and B) or MaeII (C) and hybridized to probes for endogenous C-type retrovirus repeat (A), IAP repeats (B), and major satellite repeats (C). DNA digested with MspI (M) is a control for complete lack of methylation. (n/n), a *Dnmt1* hypomorphic homozygous line, 52 (Li et al., 1992).

(D) Methylation of region 2 of *Igf2r*. Genomic DNA was digested with PvuII (P), PvuII and MspI (P/M), or PvuII and HpaII (not indicated) and hybridized to the region 2 probe.

(E) Methylation of the 5′ upstream region of *H19*. Genomic DNA was digested with SacI and HhaI or SacI alone (Sc). The right panel shows *H19* methylation in two additional [*Dnmt3a*$^{-/-}$, *Dnmt3b*$^{-/-}$] lines.

(F) Methylation of the DMR2 region of *Igf2*. Genomic DNA was digested with BamHI (B), BamHI and MspI (B/M), or BamHI and HpaII.

(G) Methylation of the 5′ region of the *Xist* gene. Genomic DNA isolated from undifferentiated ES cells (d0) or cells that were differentiated in vitro for 4, 8, and 16 days (d4, d6, d8, and d16) was digested with EcoRV and HhaI.

extensively characterized in wild-type and *Dnmt1* mutant ES cells (Tucker et al., 1996). It has been shown that an intronic CpG island, known as “region 2”, in the Igf2 receptor (*Igf2r*) gene is methylated when it is inherited from the mother, but unmethylated when it is inherited from the father (Stöger et al., 1993). We found that the region 2 sequence (presumably, of the maternal allele) in [*Dnmt3a*$^{-/-}$, *Dnmt3b*$^{-/-}$] ES cells was resistant to digestion by a methylation-sensitive restriction enzyme (Figure 6D). Similarly, the 5′ upstream region of *H19* gene was methylated in three of the four [*Dnmt3a*$^{-/-}$, *Dnmt3b*$^{-/-}$] ES cell lines (Figure 6E). The partial demethylation in one of the lines is probably fortuitous, representing clonal variation, as methylation of

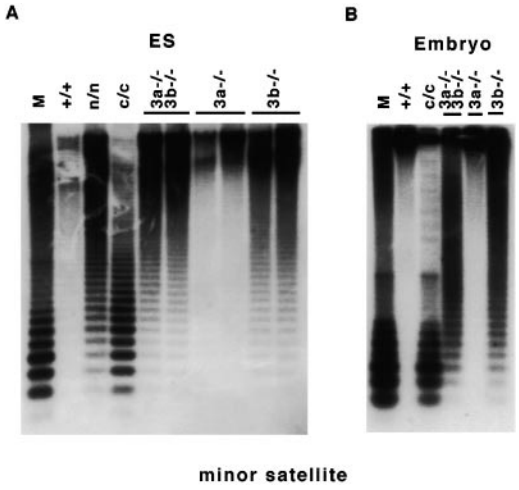

Figure 7. Methylation of Minor Satellite Repeats by Dnmt3b

Genomic DNA from ES cells (A) or embryos (B) was digested with HpaII and hybridized to the pMR150 probe. Note that minor satellite repeats were hypomethylated to the same extent in *Dnmt3b*$^{-/-}$ and [*Dnmt3a*$^{-/-}$, *Dnmt3b*$^{-/-}$] mutants.

H19 in the other three lines was stable over 20 passages (data not shown). However, to our surprise, a differentially methylated region in the *Igf2* gene, known as DMR2 (Feil et al, 1994), was almost completely demethylated in [*Dnmt3a*$^{-/-}$, *Dnmt3b*$^{-/-}$] cells, but not in the *Dnmt3a*$^{-/-}$, *Dnmt3b*$^{-/-}$, or [*Dnmt3a*$^{-/-}$, *Dnmt3b*$^{+/-}$] cells (Figure 6F). The methylation level of this region in [*Dnmt3a*$^{-/-}$, *Dnmt3b*$^{-/-}$] cells was comparable to that in *Dnmt1* null mutant cells (Figure 6F). We also analyzed methylation of the *Xist* promoter region in ES cells before and after differentiation. This region is moderately methylated in wild-type ES cells, and the methylation level increases (by de novo methylation) upon differentiation of ES cells (Figure 6G). Similar to the *Igf2* DMR2 region, the 5′ region of *Xist* was also highly demethylated in undifferentiated [*Dnmt3a*$^{-/-}$, *Dnmt3b*$^{-/-}$] cells and did not undergo de novo methylation upon differentiation in vitro. These observations suggest that some genomic sequences are subject to demethylation of unknown mechanisms, and "maintenance" of methylation patterns of these sequences in ES cells requires persistent de novo methylation by Dnmt3 proteins.

Dnmt3b Is Required for Methylation of Centromeric Minor Satellite Repeats

Despite their overlapping function in de novo methylation of various sequences in vivo, distinct functional properties of Dnmt3a and Dnmt3b are suggested by the observation that *Dnmt3a*$^{-/-}$ and *Dnmt3b*$^{-/-}$ mice displayed different development defects. This raised the possibility that Dnmt3a and Dnmt3b might methylate different sets of sequences in the genome. Minor satellite DNA consists of tandem repeats at copy numbers of 50,000–100,000, located in centromeric regions (Hastie, 1989). We showed that the minor satellite repeats were substantially demethylated in *Dnmt3b*$^{-/-}$, but not in *Dnmt3a*$^{-/-}$ ES cells (Figure 7A). Furthermore, the minor satellite repeats in [*Dnmt3a*$^{-/-}$, *Dnmt3b*$^{-/-}$] ES cells were demethylated to approximately the same level as in *Dnmt3b*$^{-/-}$ cells, suggesting that disruption of *Dnmt3a* did not contribute to the demethylation of these repeats. Similar demethylation of the minor satellite repeats was also detected in E9.5 *Dnmt3b*$^{-/-}$ and [*Dnmt3a*$^{-/-}$, *Dnmt3b*$^{-/-}$] embryos, but not in *Dnmt3a*$^{-/-}$ embryos (Figure 7B). These results suggest that the minor satellite repeats, in contrast to other repetitive sequences, are specific targets of Dnmt3b. It should be noted that the minor satellite repeats in *Dnmt1* null mutant ES cells or embryos were demethylated to levels lower than those in *Dnmt3b*$^{-/-}$ ES cells or embryos (Figures 7A and 7B), suggesting that *Dnmt3b* might contribute to methylation of a subset of minor satellite repeats.

Mutations of Human *DNMT3B* in ICF Syndrome

Recently, the human *DNMT3B* gene has been mapped to 20q11.2 (Robertson et al., 1999; Xie et al., 1999), a locus associated with ICF syndrome (*i*mmunodeficiency, *c*entromeric instability, *f*acial anomalies) (Wijmenga et al., 1998). This rare autosomal recessive disorder is characterized by variable immunological defects, centromeric heterochromatin instability, and facial anomalies (Smeets et al., 1994). DNA methylation studies have shown that the classical satellites II and III, which are major components of constitutive heterochromatin, are hypomethylated in this syndrome (Jeanpierre et al. 1993), similar to the hypomethylation of centromeric minor satellite repeats in *Dnmt3b*$^{-/-}$ mutant mice (Figure 7). This observation, together with the genetic linkage data, raised the possibility that ICF syndrome may be associated with dysfunction of DNMT3B.

To determine whether *DNMT3B* is indeed disrupted in this syndrome, we analyzed immortalized lymphoblasts derived from an affected individual and her parents (Carpenter et al., 1988). Nucleotide sequencing of the *DNMT3B* transcript from the proband revealed two mutations, consistent with a compound heterozygote. A heterozygous guanidine to adenosine mutation, resulting in a substitution of alanine to threonine at codon 603, was present in the proband and in her mother (Figure 8B). This missense mutation occurs in a region between motifs I and IV, within the catalytic domain of DNMT3B (Xie et al., 1999). A second heterozygous change in the *DNMT3B* transcript from the proband was observed at codon 744, consisting of a 9 bp insertion encoding three amino acids: serine, threonine, and proline (Figure 8C). This insertion occurred upstream of the exon 23 splice acceptor site and was derived from the adjacent intronic sequence (Xie et al., 1999). The insertion is within the conserved region of the catalytic domain, which is likely to be disrupted by insertion of a proline residue. Analysis of genomic sequence revealed a guanidine to adenosine mutation within intron 22, located 11 nucleotides 5′ to the normal splice acceptor site. This mutation results in the generation of a novel splice acceptor site (AG′TA), which is presumably responsible for the insertion of the adjacent 9 nucleotides into the altered transcript (Figure 8D). Neither the intronic mutation nor the altered *DNMT3B* transcript was present in either parent, suggesting that it may be the consequence of a de novo germline event in the proband. Analysis of immortalized lymphoblasts from 50

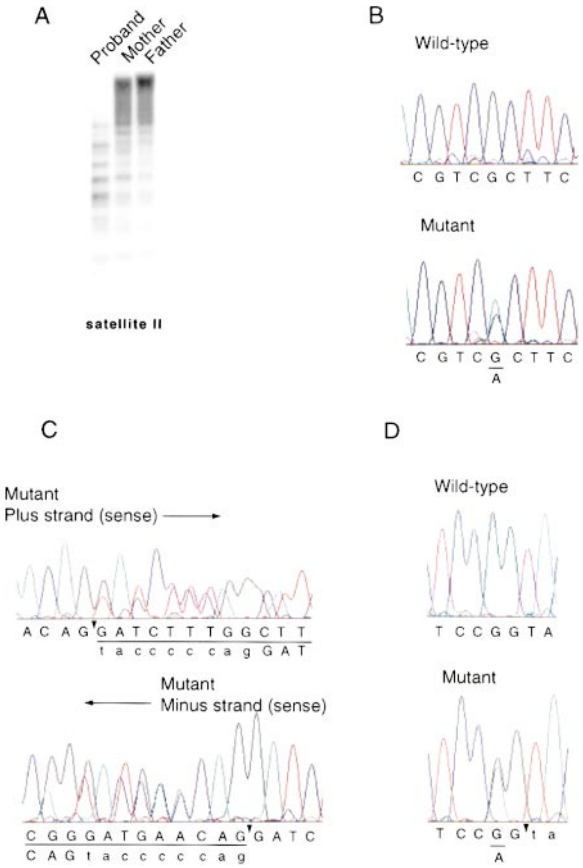

Figure 8. Mutations of *DNMT3B* in Patient with ICF Syndrome

(A) Methylation of centromeric satellites II repeats in a proband with ICF syndrome and her parents. DNA was digested with BstBI and probed using a labeled oligonucleotide specific to the satellites II repeats (Ji et al., 1997).

(B) G to A substitution at nucleotide position 1807 of *DNMT3B*, resulting in an alanine to threonine missense mutation in codon 603, detected both in the proband and her mother.

(C) Insertion within the *DNMT3B* transcript of the proband of 9 bp, encoding serine, threonine, and proline, between codons 743 and 744. The insertion is derived from the intronic sequence flanking the 5′ splice site of exon 23. Analysis of uncloned RT–PCR products shows equal representation of the wild-type and mutant transcripts in the unsynchronized sequence. In the upper panel, analysis of the plus strand shows the sequence of exon 20 (left; uppercase letters), which is normally spliced to that of exon 23 (right; uppercase letters). The arrowhead denotes the normal splice site between exons 20 and 23. Inserted intronic sequence is shown in lowercase letters. In the lower panel, analysis of the minus strand (converted to sense sequence) shows the sequence of exon 23 (right; uppercase letters) and exon 20 (left; uppercase letters) and confirms the 9 bp insertion of intronic sequence (lowercase letters).

(D) Intronic G to A substitution, 11 nucleotides 5′ of the exon 23 splice acceptor site. The mutation leads to a novel splice acceptor site (AG′TA), resulting in insertion of the adjacent nine intronic nucleotides into the *DNMT3B* transcript. The novel splice acceptor site is denoted by arrowhead, and the first two nucleotide of the insertion are in lowercase letters.

healthy individuals (i.e., 100 alleles) failed to identify either the missense mutation or the altered transcript, indicating that both mutations are unlikely to represent polymorphic variants in the population. These results, together with the chromosomal linkage and characteristic hypomethylation of centromeric repeats, suggest that mutations of *DNMT3B* are responsible for ICF syndrome.

Discussion

Dnmt3a and *Dnmt3b* Encode Functional De Novo Methyltransferases

De novo methylation and maintenance methylation are two distinct processes that are required for the establishment and mitotic inheritance of tissue-specific methylation patterns. An ongoing debate since the cloning of *Dnmt1* has been whether de novo methylation and maintenance methylation are carried out by Dnmt1 alone or by two or more distinct enzymes. Biochemical and genetic studies have demonstrated that Dnmt1 is the major maintenance methyltransferase. In this study, we show that two recently identified DNA methyltransferases Dnmt3a and Dnmt3b are essential for de novo methylation in ES cells and early embryos. Inactivation of both Dnmt3a and Dnmt3b disrupts de novo methylation of proviral DNA in ES cells (Figure 2) and genome-wide de novo methylation occurring during early development, but it has no discernible effect on the maintenance of preexisting methylation patterns (see Figure 5F). Our findings thus provide genetic evidence that *Dnmt3a* and *Dnmt3b* encode DNA methyltransferases which are primarily responsible for de novo methylation during development.

While it remains possible that Dnmt1 might be involved in de novo methylation of some unique sequences in vivo, Dnmt1 is unlikely to be the predominant de novo methyltransferase in development as was previously claimed (Yoder et al., 1997). Our observations that Dnmt1 fails to methylate retroviral DNA and various repetitive sequences de novo in ES cells and embryos lacking both Dnmt3a and Dnmt3b suggest that Dnmt1 alone probably cannot initiate de novo methylation in vivo. It is unknown why Dnmt3a and Dnmt3b can carry out de novo methylation efficiently in vivo, while they show lower methyltransferase activity than Dnmt1 in vitro (Lei et al., 1996; Okano et al., 1998b). It is possible that efficient de novo methylation by Dnmt3a and Dnmt3b requires the interaction of these proteins with other proteins or with chromatin. Further studies will be required to elucidate the mechanisms by which Dnmt3a and Dnmt3b catalyze de novo methylation in vitro and in vivo.

De Novo Methylation Is an Essential Developmental Process

Genome-wide de novo methylation occurring during early development plays a major role in the establishment of embryonic methylation patterns (Razin and Cedar, 1993). In this study, we show that inactivation of both Dnmt3a and Dnmt3b causes early embryonic lethality, demonstrating that de novo methylation is an essential process for mammalian development. As illustrated in Figure 5F, Dnmt3a and Dnmt3b carry out de novo methylation in early postimplantation embryos, resulting in a rapid increase in the methylation of bulk DNA while Dnmt1 is required for the maintenance of

all methylation in the genome. Both establishment and maintenance of a hypermethylated genome are essential for embryonic development beyond gastrulation. De novo methylation may play an important role in organizing or compartmentalizing the genome during tissue differentiation, such that tissue-specific gene expression patterns can be established. DNA methylation has been implicated in chromatin remodeling mediated by methyl CpG-binding proteins (Ng and Bird, 1999), and its disruption may result in global genomic deregulation, abrogating embryonic development. De novo methylation may also play important roles in regulation of X chromosome inactivation and genomic imprinting in mammals. Dnmt3a and Dnmt3b are likely to be responsible for de novo methylation of *Xist* (on the active X) and the CpG islands on the inactive X during X inactivation and of imprinted genes during gametogenesis. Further studies will be required to test these hypotheses.

Distinct Functions of Dnmt3a and Dnmt3b in Development and Disease

The persistent expression of *Dnmt3a* and *Dnmt3b* after gastrulation suggests that de novo methylation is not strictly confined to early embryos as previously thought. The distinct expression patterns of *Dnmt3a* and *Dnmt3b* suggest that de novo methylation may also play an important role during late development. Mice lacking either Dnmt3a or Dnmt3b display different defects and die at different stages of development (Figures 4A–4C), indicating that they have distinct functions during development. Dnmt3b may play more important roles during early development and methylate a broader spectrum of target sequences, whereas Dnmt3a may methylate a set of genes or sequences that are critical during late development or after birth.

One important observation is that Dnmt3b, but not Dnmt3a, specifically methylates the centromeric minor satellite repeats in ES cells and developing embryos (Figure 7). Although the function of methylation of centromeric repeats is unknown, our finding that *DNMT3B* is mutated in human ICF syndrome, a disease characterized by hypomethylation of centrometric satellites II and III and centromeric heterochromatin instability, suggests that methylation of centromeric repeats may play an important role in maintaining chromosome stability. It remains to be determined how these mutations might affect enzymatic activity of DNMT3B, but the fact that both mutations reside in the catalytic domain suggests that they may cause at least partial loss of function. We presume that complete loss-of-function mutations in *DNMT3B* would be lethal in humans, as it is in mice. The Dnmt3b-deficient mice may provide a useful animal model for studying cellular and developmental defects in ICF syndrome. Further studies will be required to elucidate specific roles of Dnmt3a and Dnmt3b in normal development and disease.

Experimental Procedures

Construction of Targeting Vectors

To construct *Dnmt3a* targeting vectors, a 13.5 kb ApaI-XhoI *Dnmt3a* genomic fragment was cloned into pBluescript II SK vector. A 0.3 kb ApaI-NruI fragment containing exons encoding the PC and ENV motifs was then replaced either by the IRES-βgeo cassette with the splicing accept site (Mountford et al., 1994) or a PGK-hygromycin cassette in the same transcriptional orientation as *Dnmt3a* (Figure 1A). To construct *Dnmt3b* targeting vectors, a 2.4 kb AatII-XbaI fragment containing the PC and ENV motifs was deleted from a 14 kb EcoRV-ScaI *Dnmt3b* genomic fragment in the pBluescript II SK vector and replaced by the IRES-βgeo cassette, the PGK-hygromycin cassette, or the PGK-puromycin cassette (Figure 1B). The IRES-βgeo and PGK-hygromycin cassettes were placed in the same transcriptional orientation as *Dnmt3b*, while the PGK-puromycin cassette was in the opposite orientation. All targeting vectors were linearized with NotI prior to transfection into ES cells.

Generation of Mutant ES Cell Lines and Mice

Targeting vectors for *Dnmt3a* or *Dnmt3b* with IRES-βgeo cassettes were electroporated into J1 ES cells, which were subsequently selected in G418-containing medium as described previously (Li et al. 1992). Genomic DNA isolated from G418-resistant colonies was digested with HindIII (for *Dnmt3a*) or BamHI (for *Dnmt3b*) and analyzed by Southern hybridization using a 0.3 kb SphI-ApaI fragment as a probe for *Dnmt3a*, or a 0.5 kb BamHI-HindIII fragment as a 5′ probe and 0.7 kb ScaI-BamHI fragment as a 3′ probe for *Dnmt3b* (see Figures 1A and 1B). Targeting frequency was about 80% for both *Dnmt3a* and *Dnmt3b*. Chimeric mice and F1 heterozygotes were generated from multiple Dnmt3a or Dnmt3b mutant ES cell lines as described (Li et al. 1992). Mutant mice were maintained on a 129SvJae × C57BL/6 hybrid background and analyzed.

To generate ES cell lines homozygous for *Dnmt3a* or *Dnmt3b* mutations, the second wild-type allele was disrupted with the hygromycin targeting vectors. Targeting frequency was 9/96 and 11/154 for *Dnmt3a* and *Dnmt3b*, respectively. *Dnmt3a* homozygous lines were also generated by selection of heterozygous (βgeo/+) cells in medium containing high concentration of G418 (6 mg/ml active form) for 14 days. Of 96 resistant colonies, eight were found to be homozygous for *Dnmt3a* mutation (βgeo/βgeo). To generate ES cell lines lacking both Dnmt3a and Dnmt3b, the *Dnmt3a* homozygous (βgeo/βgeo) ES cells were subject to two sequential rounds of gene targeting using *Dnmt3b* targeting vectors containing hygromycin and puromycin. The targeting frequency was 19/154 and 20/96 for hygromycin and puromycin vectors, respectively.

Infection of ES Cells with Retrovirus

Infection of wild-type and *Dnmt3a* or *Dnmt3b* mutant ES cells with the MoMuLV^{sup}-1 virus, DNA preparation, and analysis of de novo methylation of newly integrated provirus were carried out as described (Lei et al., 1996), except that single infection for 6 hr instead of multiple rounds of infection was done.

DNA Preparation and Methylation Analysis

Blastocysts were collected from superovulated C57BL/6 females after mating with C57BL/6 male mice using the standard protocol (Hogan et al. 1994). DNA from about 100 blastocysts was digested and loaded on one lane (Figures 5D and 5E). DNA from embryos, yolk sac, and cell lines was isolated, digested with methylation-sensitive or -insensitive enzymes, and analyzed by Southern hybridization as previously described (Lei et al., 1996). Probes for methylation analysis include the following: πAN7 for *supF* of MoMuLV^{sup}-1 (Lei et al., 1996); pMO for endogeous C-type retroviruses (Li et al., 1992); pSAT for major satellite repeats (gift from A. Bird); pMR150 for minor satellite repeats (Chapman et al., 1984); IAP (Walsh et al., 1998); the *Igf2r* region 2 probe (Stöger et al., 1993); the *H19* upstream region (Tremblay et al., 1995); DMR2 or "probe 6" for *Igf2* (Feil et al., 1994); 5′ region of *Xist* cDNA (gift from T. Sado); and an oligonucleotide probe (5′-TCGAGTCCATTCGATGAT-3′) specific to human classic satellite II (Ji et al., 1997).

RNA Preparation and Northern Analysis

Total RNA prepared from ES cells was analyzed using standard Northern hybridization protocols. *Dnmt3a*- and *Dnmt3b*-specific probes were a 1.05 kb (nt 2615–nt 3661, AF068625) fragment and a 1.0 kb EST clone (AA116694), respectively. Both probes overlap with the C-terminal catalytic domain. The *Oct3/4* probe was a 720 bp cDNA fragment obtained by RT–PCR.

Immunoblot Analysis

ES cells were lysed in SDS loading buffer and quickly heated at 70°C for 15 min. The cell lysates were fractionated by SDS–PAGE (8%) and blotted onto nitrocellulose membrane (Millipore). Immunoblot was carried out using anti-Dnmt1 antibody, pATH56, as described (Li et al., 1992).

Whole-Mount X-Gal Staining and Histology

Male mice heterozygous for either *Dnmt3a* or *Dnmt3b* mutation were crossed with wild-type or heterozygous female. Embryos at E7.5–E9.5 were dissected out of decidua, fixed, stained with X-gal, and analyzed by histology as described (Hogan et al., 1994). Embryos were sectioned at 7 μm and counterstained with nuclear fast red.

Analysis of Mutations in the Human *DNMT3B* Gene

For mutational analysis of patients with ICF syndrome, EBV immortalized lymphoblasts were obtained from Coriell Cell Repositories of the NIGMS Human Genetic Mutant Cell Repository. GM08714, proband; GM08728, mother; and GM08729, father. Total cellular RNA was extracted using the GTC-$CsCl_2$ method. Uncloned RT–PCR products spanning overlapping fragments of the transcript were sequenced in both directions, using Energy Transfer Dye Primer (Amersham), and analyzed for the presence of heterozygous mutations. Genomic sequences flanking exon 23 were PCR-amplified and sequenced. (For intron/exon junctions, see Xie et al., 1999.) Exons 10, 21, and 22, which are alternatively spliced, were also amplified from genomic DNA and sequenced. To determine whether mutations in *DNMT3B* were present in a control population, RT–PCR products from EBV immortalized lymphoblasts derived from 50 healthy individuals were analyzed using DHPLC chromatography (Transgenomic) (Liu et al., 1998).

Acknowledgments

We thank H. Lei and L. Yu for excellent technical assistance and Dr. D. Barlow, Dr. M. Bartolomei, Dr. A. Bird, Dr. P. Laird, Dr. W. Reik, Dr. J. Rossant, Dr. A. Smith, and Dr. S. Tilghman for various plasmid DNA and probes, Dr. T. Bestor for anti-Dnmt1 antibody, and Dr. R. Chen for puromycin-resistant MEF cells. This work is supported by grants from National Institutes of Health (GM52106, CA82389) and Bristol Myers-Squibb (E. L.) and by a grant from the Center for Cancer Risk Analysis (D. H.), Massachusetts General Hospital. M. O. was supported by the Japan Society for the Promotion of Science and is a special fellow of Leukemia Society of America.

Received September 27, 1999; revised October 12, 1999.

References

Bestor, T.H. (1992). Activation of mammalian DNA methyltransferase by cleavage of a Zn binding regulatory domain. EMBO J. *11*, 2611–2617.

Bestor, T.H., Laudano, A.P., Mattaliano, R., and Ingram, V.M. (1988). Cloning and sequencing of a cDNA encoding DNA methyltransferase of mouse cells. The carboxyl-terminal domain of the mammalian enzymes is related to bacterial restriction methyltransferases. J. Mol. Biol. *203*, 971–983.

Brockdorff, N. (1997). Convergent themes in X chromosome inactivation and autosomal imprinting. In Genomic Imprinting: Frontiers in Molecular Biology, W. Reik and A. Sorani, eds. (Oxford: IRL Press), pp. 191–210.

Carpenter, N.J., Filipovich, A., Blaese, R.M., Carey, T.L., and Berkel, A.I. (1988). Variable immunodeficiency with abnormal condensation of the heterochromatin of chromosomes 1, 9, and 16. J. Pediatr. *112*, 757–760.

Chaillet, J.R., Vogt, T.F., Beier, D.R., and Leder, P. (1991). Parental-specific methylation of an imprinted transgene is established during gametogenesis and progressively changes during embryogenesis. Cell *66*, 77–83.

Chapman, V., Forrester, L., Sanford, J., Hastie, N., and Rossant, J. (1984). Cell lineage-specific undermethylation of mouse repetitive DNA. Nature *307*, 284–286.

Colot, V., and Rossignol, J.L. (1999). Eukaryotic DNA methylation as an evolutionary device. Bioessays *21*, 402–411.

Ehrlich, M. (1999). DNA hypomethylation and cancer. In DNA Alterations in Cancer: Genetic and Epigenetic Changes, M. Ehrlich, ed. (Natick, MA: BioTechniques Books).

Feil, R., Walter, J., Allen, N.D., and Reik, W. (1994). Developmental control of allelic methylation in the imprinted mouse Igf2 and H19 genes. Development *120*, 2933–2943.

Hastie, N.D. (1989). Highly repeated DNA families in the genome of Mus musculus. In Genetic Variants and Strains of the Laboratory Mouse, Second Edition, M.F. Lyon and A.G. Searle, eds. (Oxford: Oxford University Press), pp. 559–573.

Hogan, B., Beddington, R., Costantini, F., and Lacy, E. (1994). Manipulating the Mouse Embryo, Second Edition (Cold Spring Harbor, NY: Cold Spring Harbor Laboratory Press).

Holliday, R., and Pugh, J.E. (1975). DNA modification mechanisms and gene activity during development. Science *187*, 226–232.

Howlett, S.K., and Reik, W. (1991). Methylation levels of maternal and paternal genomes during preimplantation development. Development *113*, 119–127.

Jähner, D., and Jaenisch, R. (1984). DNA methylation in early mammalian development. In DNA Methylation: Biochemistry and Biological Significance, A. Razin, H. Cedar, and A. Riggs, eds. (New York: Springer-Verlag), pp. 189–219.

Jähner, D., Stuhlmann, H., Stewart, C.L., Harbers, K., Löhler, J., Simon, I., and Jaenisch, R. (1982). De novo methylation and expression of retroviral genomes during mouse embryogenesis. Nature *298*, 623–628.

Jeanpierre, M., Turleau, C., Aurias, A., Prieur, M., Ledeist, F., Fischer, A., and Viegas-Péquignot, E. (1993). An embryonic-like methylation pattern of classical satellite DNA is observed in ICF syndrome. Hum. Mol. Genet. *2*, 731–735.

Ji, W., Hernandez, R., Zhang, X.Y., Qu, G.Z., Frady, A., Varela, M., and Ehrlich, M. (1997). DNA demethylation and pericentromeric rearrangements of chromosome 1. Mutat. Res. *379*, 33–41.

Jones, P.A., and Laird, P.W. (1999). Cancer epigenetics comes of age. Nat. Genet *21*, 163–167.

Kafri, T., Ariel, M., Brandeis, M., Shemer, R., Urven, L., McCarrey, J., Cedar, H., and Razin, A. (1992). Developmental pattern of gene-specific DNA methylation in the mouse embryo and germ line. Genes Dev. *6*, 705–714.

Kumar, S., Cheng, X., Klimasauskas, S., Mi, S., Posfai, J., Roberts, R., and Wilson, G.G. (1994). The DNA (cytosine-5) methyltransferases. Nucleic Acids Res. *22*, 1–10.

Lei, H., Oh, S.P., Okano, M., Jüttermann, R., Goss, K.A., Jaenisch, R., and Li, E. (1996). De novo DNA cytosine methyltransferase activities in mouse embryonic stem cells. Development *122*, 3195–3205.

Leonhardt, H., Page, A.W., Weier, H.-U., and Bestor, T.H. (1992). A targeting sequence directs DNA methyltransferase to sites of DNA replication in mammalian nuclei. Cell *71*, 865–873.

Li, E. (1997). Role of DNA methylation in development. In Genomic Imprinting: Frontiers in Molecular Biology, W. Reik and A. Surani, eds. (Oxford: IRL Press), pp. 1–20.

Li, E., Bestor, T.H., and Jaenisch, R. (1992). Targeted mutation of the DNA methyltransferase gene results in embryonic lethality. Cell *69*, 915–926.

Liu, W., Smith, D.I., Rechtzigel, K.J., Thibodeau, S.N., and James, C.D. (1998). Denaturing high performance liquid chromatography (DHPLC) used in the detection of germline and somatic mutations. Nucleic Acids Res. *26*, 1396–1400.

Monk, M., Boubelik, M., and Lehnert, S. (1987). Temporal and regional changes in DNA methylation in the embryonic, extraembryonic and germ cell lineages during mouse embryo development. Development *99*, 371–382.

Mountford, P., Zevnik, B., Duwel, A., Nichols, J., Li, M., Dani, C., Robertson, M., Chambers, I., and Smith, A. (1994). Dicistronic targeting constructs: reporters and modifiers of mammalian gene expression. Proc. Natl. Acad. Sci. USA *91*, 4303–4307.

Ng, H.H., and Bird, A. (1999). DNA methylation and chromatin modification. Curr. Opin. Genet. Dev. *9*, 158–163.

Okano, M., Xie, S., and Li, E. (1998a). Dnmt2 is not required for de novo and maintenance methylation of viral DNA in embryonic stem cells. Nucleic Acids Res. *26*, 2536–2540.

Okano, M., Xie, S., and Li, E. (1998b). Cloning and characterization of a family of novel mammalian DNA (cytosine-5) methyltransferases. Nat. Genet. *19*, 219–220.

Palmiter, R.D., Chen, H.Y., and Brinster, R.L. (1982). Differential regulation of metallothionein-thymidine kinase fusion genes in transgenic mice and their offspring. Cell *29*, 701–710.

Razin, A., and Cedar, H. (1993). DNA methylation and embryogenesis. In DNA Methylation: Molecular Biology and Biological Significance, J.P. Jost and H.P. Saluz, eds. (Basel: Birkhäuser Verlag), pp. 343–357.

Riggs, A.D. (1975). X inactivation, differentiation, and DNA methylation. Cytogenet. Cell Genet. *14*, 9–25.

Robertson, K.D., Uzvolgyi, E., Liang, G., Talmadge, C., Sumegi, J., Gonzales, F.A., and Jones, P.A. (1999). The human DNA methyltransferases (DNMTs) 1, 3a and 3b: coordinate mRNA expression in normal tissues and overexpression in tumors. Nucleic Acids Res. *27*, 2291–2298.

Sanford, J.P., Clark, H.J., Chapman, V.M., and Rossant, J. (1987). Differences in DNA methylation during oogenesis and spermatogenesis and their persistence during early embryogenesis in the mouse. Genes Dev. *1*, 1039–1046.

Smeets, D.F., Moog, U., Weemaes, C.M., Vaes-Peeters, G., Merkx, G.F., Niehof, J.P., and Hamers, G. (1994). ICF syndrome: a new case and review of the literature. Hum. Genet. *94*, 240–246.

Stein, R., Gruenbaum, Y., Pollack, Y., Razin, A., and Cedar, H. (1982). Clonal inheritance of the pattern of DNA methylation in mouse cells. Proc. Natl. Acad. Sci. USA *79*, 61–65.

Stewart, C., Stuhlmann, H., Jähner, D., and Jaenisch, R. (1982). De novo methylation, expression, and infectivity of retroviral genomes introduced into embryonal carcinoma cells. Proc. Natl. Acad. Sci. USA *79*, 4098–4102.

Stöger, R., Kubicka, P., Liu, C.G., Kafri, T., Razin, A., Cedar, H., and Barlow, D.P. (1993). Maternal-specific methylation of the imprinted mouse Igf2r locus identifies the expressed locus as carrying the imprinting signal. Cell *73*, 61–71.

Surani, M.A. (1998). Imprinting and the initiation of gene silencing in the germline. Cell *93*, 309–312.

Tremblay, K.D., Saam, J.R., Ingram, R.S., Tilghman, S.M., and Bartolomei, M.S.A. (1995). paternal-specific methylation imprinting marks the alleles of the mouse H19 gene. Nat. Genet. *9*, 407–413.

Tucker, K.L., Beard, C., Dausmann, J., Jackson-Grusby, L., Laird, P.W., Lei, H., Li, E., and Jaenisch, R. (1996). Germ-line passage is required for establishment of methylation and expression patterns of imprinted but not of nonimprinted genes. Genes Dev. *10*, 1008–1020.

Walsh, C.P., Chaillet, J.R., and Bestor, T.H. (1998). Transcription of IAP endogenous retroviruses is constrained by cytosine methylation. Nat. Genet. *20*, 116–117.

Wigler, M., Levy, D., and Perucho, M. (1981). The somatic replication of DNA methylation. Cell *24*, 33–40.

Wijmenga, C., van den Heuvel, L.P., Strengman, E., Luyten, J.A., van der Burgt, I.J., de Groot, R., Smeets, D.F., Draaisma, J.M., van Dongen, J.J., De Abreu, R.A., et al. (1998). Localization of the ICF syndrome to chromosome 20 by homozygosity mapping. Am. J. Hum. Genet. *63*, 803–809.

Xie, S., Wang, Z., Okano, M., Nogami, M., Li, Y., He, W.W., Okumura, K., and Li, E. (1999). Cloning, expression and chromosome locations of the human DNMT3 gene family. Gene *236*, 87–95.

Yoder, J.A., Soman, N.S., Verdine, G.L., and Bestor, T.H. (1997). DNA (cytosine-5)-methyltransferases in mouse cells and tissues. Studies with a mechanism-based probe. J. Mol. Biol. *270*, 385–395.